Multivalency in lectins – A crystallographic, modelling and light-scattering study involving peanut lectin and a bivalent ligand

S. Kundhavai Natchiar[1], O. Srinivas[2], Nivedita Mitra[1], Sagarika Dev[1], N. Jayaraman[2], A. Surolia[1] and M. Vijayan[1,*]

[1]Molecular Biophysics Unit and [2]Department of Organic Chemistry, Indian Institute of Science, Bangalore 560 012, India

Multivalency is believed to be important in the activity of lectins, although definitive structural studies on it have been few and far between. We have now studied the complexation of tetravalent peanut lectin with a synthetic compound containing two terminal lactose moieties, using a combination of crystallography, dynamic light scattering and modelling. Light scattering indicates the formation of an apparent dimeric species and also larger aggregates of the tetrameric lectin in the presence of the bivalent ligand. Crystals of presumably crosslinked lectin molecules could be obtained. They diffract poorly, but X-ray data from them are good enough to define the positions of the lectin molecules. Extensive modelling on possible crosslinking modes of protein molecules by the ligand indicated that systematic crosslinking could lead to crystalline arrays. The studies also provided a rationale for crosslinking in the observed crystal structure. The results obtained provide further insights into the general problem of multivalency in lectins. They indicate that crosslinking involving multivalent lectins and multivalent carbohydrates could lead to an ensemble of a finite number of distinct periodic arrays rather than a unique array.

Keywords: Crosslinking, crystalline array, crystal structure prediction, lectin–carbohydrate interactions, ligand specificity.

LECTINS are multivalent carbohydrate-binding proteins, which exert their biological effects through the ability to specifically bind different sugar structures[1–4]. Although originally isolated from plant sources, they are found in different forms of life such as animals, plants, bacteria and viruses. Multivalency is believed to be important in the activity of lectins. For example, the biological activities of galectins, which are believed to include control of cell growth, activation of inflammatory cells and regulation of apoptosis, are suggested to be related to their multivalent binding properties[5]. However, only a few definitive structural studies on the multivalency of lectins have been reported so far[5–8]. An obvious tool for such studies has been multivalent saccharides. In early structural studies involving such saccharides, infinite chains of a C-type mannose-binding protein[9] and galectin-1 crosslinked by biantennary saccharides were observed[10]. Obviously, when the lectin and sugar are bivalent, such one-dimensional assemblies, often referred to as type-I crosslinked complexes, result[7,9]. However, networks (type-II complexes) result when the lectin or sugar has a valency of more than two, as in the crystal structures of complexes of soybean agglutinin with biantennary sugars[11,12]. The situation is similar in some of crystal structures of complexes of snowdrop lectin[13] and the Flt3 receptor interacting lectin[14]. A more complex situation involving a hexavalent lectin and a trivalent sugar was explored in this laboratory using modelling[15]. Here we report the study of the complexation of tetravalent peanut lectin with a synthetic compound containing two terminal carbohydrate molecules, using a combination of crystallography, dynamic light scattering and modelling. The modelling *inter alia* seeks to predict crystal structures, a problem of considerable current interest, and also to rationalize the observed crystal structure.

Peanut agglutinin (PNA) is a tetrameric lectin (Figure 1) with galactose-specificity at the monosaccharide level. Its structure and interactions with lactose, C-lactose, T-antigenic disaccharide, *N*-acetyllactosamine and methyl-*b*-galactose have been thoroughly characterized crystallographically[16–20]. A lactose-bearing bivalent azobenzene derivative, which may be called for convenience lactose–azobenzene–lactose (LAL, Figure 2), binds PNA with an order of magnitude higher affinity than lactose. Furthermore, the binding has been shown to be cooperative[21,22]. It is the type-II complexation between PNA and LAL that is reported here. The results obtained may be of considerable general interest in relation to the multivalency of lectins and rationalization of crystal structure.

Material and methods

PNA was prepared and LAL synthesized as described by Banerjee *et al.*[16] and Srinivas *et al.*[21] respectively.

*For correspondence. (e-mail: mv@mbu.iisc.ernet.in)

Crystallization

Crystallization experiments using a solution containing 0.12 mM PNA and 0.54 mM LAL in 0.05 M phosphate buffer, pH 7.0, were carried out employing the hanging drop method. In these experiments, the reservoir contained 50 mM phosphate buffer, pH 7.0 and 12% PEG 8 K. The drop contained 4 to 5 µl of protein-LAL solution and an equal volume of reservoir solution. The drop was equilibrated against the reservoir solution.

Data collection

X-ray data were collected at room temperature using an MAR research imaging plate mounted on a Rigaku rotating anode generator. Data were processed using DENZO and scaled using SCALEPACK in the HKL suite of programs[23]. Details of data collection statistics are given in Table 1. The processed data were truncated using the program[24] TRUNCATE of CCP4.

Structure solution and refinement

The structure of the PNA–LAL complex was solved using the molecular replacement program AMoRe[25]. The dimers AD and BC in the PNA–lactose complex (2PEL)[16] were used as the search model. A unique solution was obtained with CC and R-factor 0.67 and 45.7% respectively. Rigid body refinement was carried out[24] using REFMAC of CCP4[24]. The refinement parameters are given in Table 1. Coordinates of *a*-carbon positions are deposited in the Protein Data Bank (ref: 2DH1).

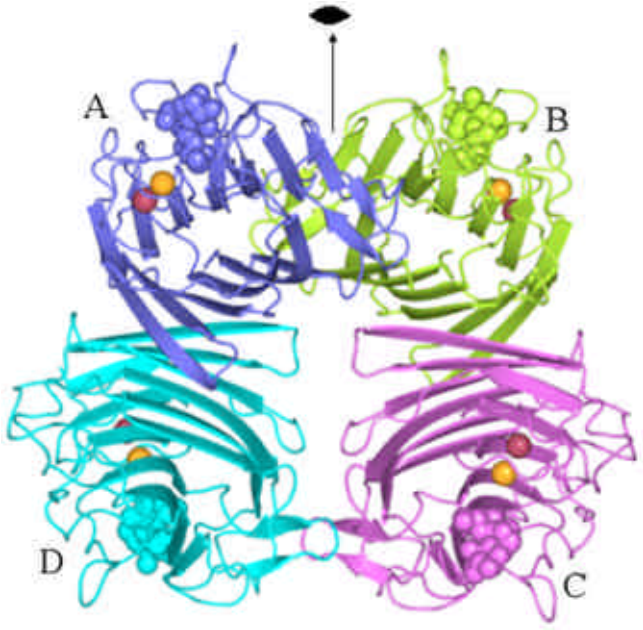

Figure 1. Structure of PNA with bound lactose in van der Waals representation. The four subunits are indicated by A, B, C and D. Magenta and yellow balls represent Mn and Ca ions respectively.

Dynamic light scattering

Before each experiment, PNA was centrifugated at 10,000 rev min^{-1} for 15 min at 4°C. The solution of the PNA–LAL complex was filtered using Whatman membrane with the pore size 0.1 µm. In the experiments, concentration of the protein was kept constant as 10 µM and molarity of LAL was varied. In each experiment, 50 measurements were made during an hour. Each measurement consisted of 15 acquisitions. DLS experiments were carried out using a Dyanpro Molecular Sizing Instrument, and the collected data were analysed using Dynamic V6 software.

Modelling

Models were built using INSIGHTII. The built carbohydrates were docked to the binding site by superposing the lactose moiety in the LAL onto the bound lactose in the PNA–lactose complex[16] (2PEL) using ALIGN[26]. Interatomic contacts were calculated using program[24] CONTACT of CCP4. Figures 1, 3–5 were prepared using PYMOL[27]. Figure 6 was generated using MOLSCRIPT[28].

Results and discussion

Light scattering

The higher affinity and cooperativity of PNA–LAL binding were suspected to arise from aggregation through cross-linking. However, it was important to experimentally explore if PNA molecules aggregate when complexed with LAL. This was done using dynamic light scattering. The results of these experiments are given in Table 2. The results of a typical experiment, along with those of protein alone in the solution, are illustrated in Figure 7. Table 2 and Figure 7 clearly show that PNA molecules aggregate in the presence of LAL. From the apparent molecular weights calculated using hydrodynamic radii, the predominant species

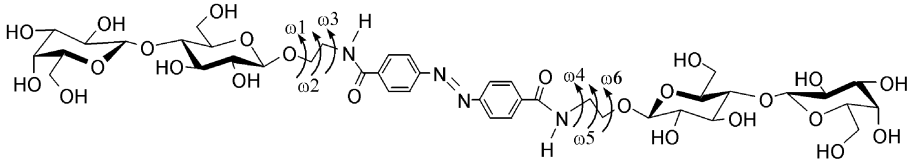

Figure 2. Structural formula of bivalent ligand (LAL). Torsion angles that define conformation of the molecule are also indicated.

appears to be a dimer of tetrameric molecules even in the presence of excess LAL. The next higher aggregate appears to involve around a hundred tetrameric molecules. No attempt at detailed analysis of light scattering was made, as it is not germane to the main theme of the investigation. The attempt primarily was only to demonstrate the aggregation of PNA molecules, presumably by crosslinking, in the presence of LAL.

Table 1. Data collection and refinement statistics

Space group	$I4_1$
Unit cell parameters	
a (Å)	92.574
b (Å)	92.574
c (Å)	473.551
Resolution (Å)	7.65
Last shell resolution (Å)	7.65–7.91
No. of observations	18464 (1782)
No. of unique reflections	2273 (219)
Completeness (%)	99.8 (100)
R_{merge} (%)	10.0 (49.0)
Multiplicity	8.1 (8.1)
R-factor (%)	35.5
R_{free} (%)	37.7
Resolution range (Å)	20.0–7.65

Values in parentheses correspond to the last resolution shell.

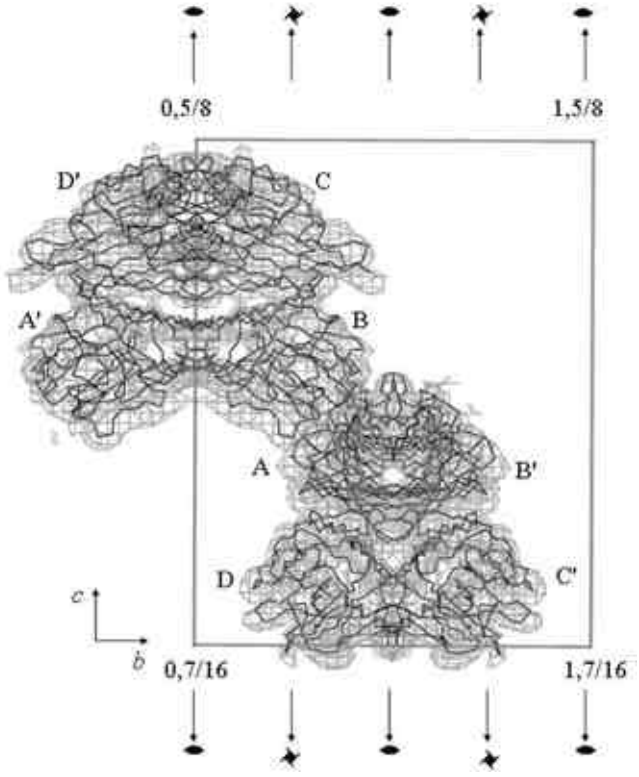

Figure 3. Superposition of PNA molecules on electron density. Contours in the 2*Fo*-*Fc* map are drawn at 1*s* level. Nomenclature of the two tetramers is indicated.

Crystal structure

In the presence of LAL, peanut lectin crystals grew in the tetragonal space group $I4_1$. In the absence of LAL, under similar conditions at neutral pH, PNA always crystallized in space group $P2_12_12$ irrespective of the ligand in the medium[16–19]. The only other space group in which PNA crystallizes is $P2_1$, at lower pH[19,20]. Over a dozen PNA crystals with different ligands bound to the lectin and grown under different environmental conditions have been studied crystallographically[16–20]. All of them belong to one of the two space groups mentioned above, depending mainly on the pH of the medium[20]. Therefore, it is reasonable to assume that the tetragonal crystals obtained in the present study

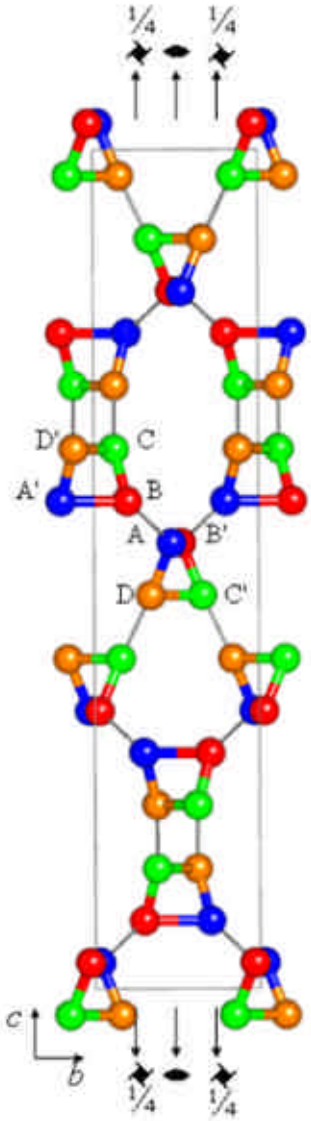

Figure 4. Schematic representation of crystal structure of the PNA–LAL complex. In this and subsequent relevant figures subunits A, B, C and D are represented respectively, blue, red, green and yellow balls. For clarity, twofold axes at $x = 0$ and 1 are not indicated. Sugar linkages are indicated by thin lines.

resulted from the presence of LAL in the medium. It is also probable that the PNA molecules are crosslinked by LAL. Furthermore, most of the PNA crystals studied so far diffracted to resolutions better than 3 Å. The tetragonal crystals diffract only to a resolution of 7.65 Å. Reduction in resolution could well have been caused by crosslinking, especially as many modes of crosslinking are possible.

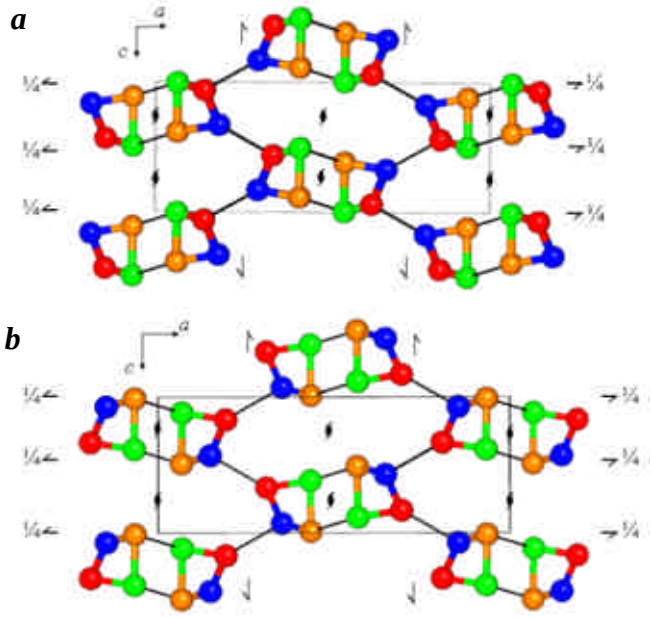

Figure 5 ***a***, ***b***. Two crystal structures constructed using LAL linkages with idealized geometries.

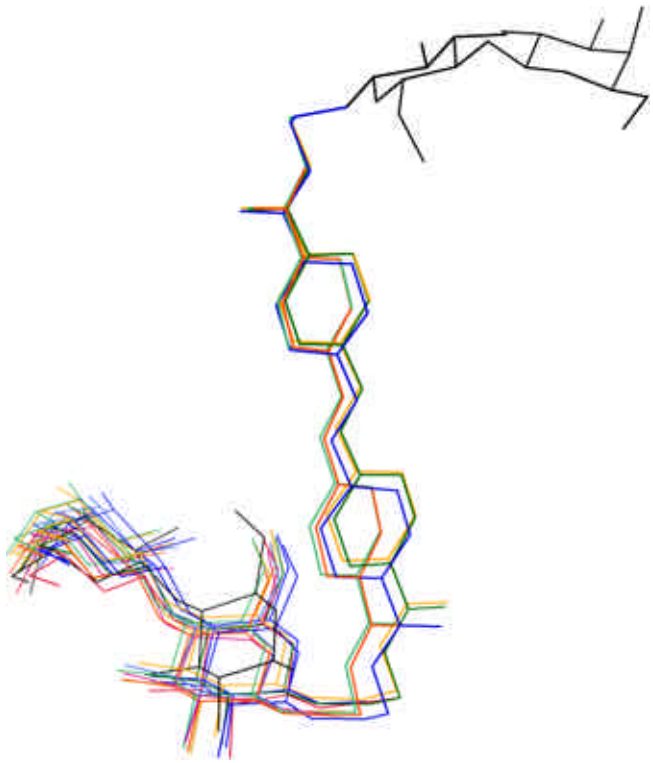

Figure 6. Superposition of LAL conformers corresponding to AB linkage in the observed crystal structure.

A resolution of 7.65 Å is admittedly not good enough to define the fine features of the structure. However, as indicated, for example, by the ready unambiguous solution of the structure obtained from molecular replacement calculations[25], it is adequate to define the positions of the molecules and the subunits in them, as is often done in conjuction electron microscopic and diffraction experiments[29,30]. Also the R and R_{free} values obtained in the present case are comparable to those obtained in the X-ray structure determinations of protein at comparable resolutions[31]. The electron density shown in Figure 3 provides a clear representation of the overall size and shape of the molecule and known detailed structure of the molecule can be readily built into it. It, along with the results of refinement, also indicates that the quaternary structure of PNA has not suffered any distortion on account of crosslinking. Four simulated annealing omit maps, calculated by omitting one of the four subunits in the asymmetric part at a time, confirmed the correctness of the interpretation.

A schematic representation of the crystal structure is shown in Figure 4. The two crystallographically independent tetramers (referred as molecule AB′C′D and molecule A′BCD′) in the structure are located on separate twofold axes, such that the asymmetric unit contains two half-tetramers involving four subunits. Not surprisingly, at this resolution the crosslinking LAL molecules are not clearly visible in the electron density, but the pattern of crosslinking can be surmised with reasonable certainty on the basis of different distances involving centroids of the subunits and galactose moiety of the bound sugar, modelled on the basis of several known PNA–sugar complexes. The surmised pattern is also indicated in Figure 4. The pattern involves two crystallographically independent linkages, one between subunit A of molecule AB′C′D and subunit B of molecule A′BCD′, and the other between subunit C of the molecule AB′C′D and subunit D of a symmetry equivalent molecule of A′BCD′. The distances between the centroids of the two tetramers, the two subunits and the two bound galactose moieties are 84.4, 42.4 and 19.9 Å in the AB link. The corresponding distances in the CD link are 80.1, 39.6 and 22.8 Å. The two links and their symmetry equivalents give rise to an array constituting the crystal.

Modelling

Modelling studies on PNA–LAL linkages have two related primary objectives. One is to explore whether linkages, when systematically made, would lead to crystalline arrays. The second is to rationalize the observed crystal structure. The peanut lectin molecule consists of four subunits, A, B, C and D (Figure 1), each carrying a binding site for, in the present context, lactose. Therefore, a linkage between two PNA tetramers could involve 16 possibilities. However, on account of the internal symmetry of

Table 2. Summary of particle size distribution in PNA–LAL solution. Concentration of PNA was maintained at 10 μM

Concentration of LAL (μM)	Hydrodynamic radius *R* (in nm)	Polydispersity (% Cp)	Per cent intensity	Apparent molecular weight*
0.0	3.7 ± 0.04	13.15 ± 0.30	90.19 ± 1.00	1.0
7.5	4.95 ± 0.14	19.97 ± 1.66	71.38 ± 1.92	2.1
	24.88 ± 1.34	11.93 ± 1.00	18.98 ± 0.82	105.1
10.0	4.89 ± 0.06	16.10 ± 1.33	75.13 ± 1.15	1.9
	21.76 ± 1.18	11.09 ± 0.89	23.54 ± 1.22	80.0
15.0	5.08 ± 0.08	17.97 ± 1.43	70.14 ± 1.25	2.1
	23.12 ± 1.23	12.24 ± 1.07	24.23 ± 1.11	86.6
30.0	5.64 ± 0.09	24.23 ± 1.23	76.47 ± 1.38	2.7
	26.28 ± 1.32	15.30 ± 0.81	19.31 ± 0.78	115.5
45.0	5.21 ± 0.06	18.61 ± 1.00	77.23 ± 0.82	2.3
	25.22 ± 0.97	13.84 ± 0.95	21.24 ± 0.64	99.0
80.0	5.35 ± 0.08	20.18 ± 1.68	82.78 ± 0.96	2.4
	26.47 ± 1.29	12.92 ± 0.85	17.58 ± 0.92	117.9
120.0	5.04 ± 0.09	16.49 ± 1.19	75.27 ± 1.25	2.1
	23.05 ± 1.10	12.96 ± 0.81	21.78 ± 0.83	85.0
160.0	5.07 ± 0.11	19.25 ± 1.39	76.77 ± 1.27	2.2
	22.07 ± 1.16	14.17 ± 0.97	21.80 ± 0.92	78.5
240.0	4.34 ± 0.17	12.55 ± 0.86	55.59 ± 1.90	1.6
	24.05 ± 0.69	10.78 ± 0.88	39.96 ± 1.18	82.3
320.0	4.65 ± 0.15	18.88 ± 1.27	72.94 ± 1.69	1.8
	20.08 ± 0.97	11.74 ± 1.05	21.86 ± 1.17	62.1
400.0	4.84 ± 0.21	17.46 ± 1.08	69.02 ± 2.26	2.2
	23.99 ± 1.49	10.98 ± 1.01	18.34 ± 0.90	104.5

*In terms of apparent molecular weight of a tetrameric molecule of PNA.

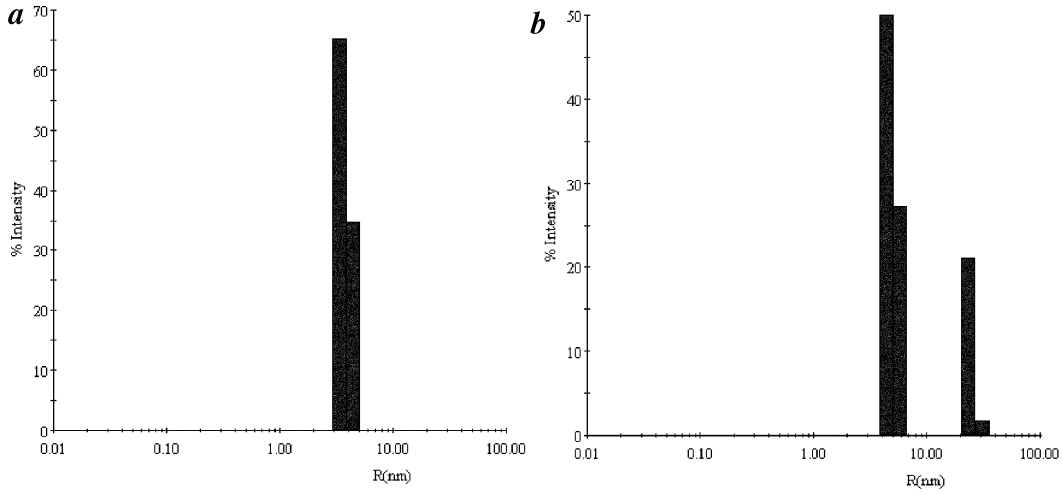

Figure 7. Result of a typical DLS measurement involving (***a***) PNA alone and (***b***) PNA and LAL in 10 : 45 molar ratio (see Table 2).

the molecule, which relates A to B and C to D, combinations AA, BB, AB and BA are equivalent; so are CC, DD, CD and DC, and AC, AD, BC, BD, CA, DA, CB and DB. Therefore, essentially only three combinations need to be considered.

LAL is a long molecule with considerable conformational flexibility. The lactose moieties at the two ends were assumed to have the same geometry as in the original PNA–lactose (2PEL) complex[16]. The O-methyl group in both cases was fixed using average values of the appropriate parameters observed in proteins complexed with methylated *b*-D-lactose or methylated *b*-D-glucose derivatives, as these parameters did not exhibit unreasonable scatter. That leaves six torsion angles, designated as *w*1 to *w*6 (Figure 2), as the variable parameters. Four of them involve rotations about C/O(sp^3)–C(sp^3) bonds and each torsion angle can have favoured values around –60, 60 and 180°; the remaining two represent rotations about C(sp^3)–

$N(sp^2)$ bonds and can have values in the neighbourhood of –90, 90 and 180°. It is reasonable to expect a variation of at least within ± 30° about each ideal value. If calculations were performed at a 10° grid interval, a full conformational analysis would involve the examination of 21^6 (≈ 86 million) possibilities. Even after effective reductions due to the chemical equivalence of the two halves of the molecule, the number of possibilities to be explored remains formidable. Attempts were made to energy-minimize the structure of LAL to arrive at a few favoured conformations, but these attempts did not lead to unambiguous results. Therefore, it was decided to use, at least to start with, only idealized conformations. In any case, the overall aim was not to enumerate all the possible crystalline arrays, but only to explore the possibility of systematic cross-linking resulting in crystalline arrays.

Generation of periodic arrays: $w1$, $w2$ and $w3$ can each assume three idealized values, resulting in a total of 27 idealized conformations for one half of the molecule. Likewise, the other half of the molecule can also have 27 idealized conformations. The total number of possible idealized conformations for the molecule is 729. In each case, the lactose group at one end of the LAL molecule was placed in the binding site of subunit A of the PNA molecule using the known geometry of the PNA–lactose complex. Another PNA molecule was moved to the other end of LAL, such that subunit B of that molecule interacted as in the PNA–lactose complex, with the lactose moiety at that end of LAL. The operation was repeated for CD (subunit C of one PNA tetramer and subunit D of the tetramer) and AC linkages as well. Thus, there were 2187 pairs of linked PNA tetramers. Linked pairs with 100 or more non-bonded atom–atom contact distances of less than 2.3 Å were eliminated from the list. Thus 410 AB linkages, 303 CD linkages and 368 AC linkages were acceptable on the basis of this criterion. On account of the symmetry in the molecular formula of LAL, in a given type of linked pair, two conformations in which $w1$, $w2$, $w3$, $w4$, $w5$ and $w6$ in one half have the same values as $w6$, $w5$, $w4$, $w3$, $w2$ and $w1$ in the other, are identical except for a switch of PNA molecules within the pair. Therefore, only one of them needs to be considered. Once this is done, the number of AB, CD and AC pairs came down to 213, 159 and 175 respectively.

If the twofold symmetry of the PNA molecule is systematically applied, each linked pair leads to an array as schematically illustrated in Figure 8 *a* for AB linkages. The same is true of CD and AC linkages. However, only a linear array is compatible with a crystalline arrangement. Referring to Figure 8 *a*, if the angle 1-2-3, defined as the angle subtended by the centroids of tetramers 1 and 3 at the centroid of 2, is close to 180°, one obtains a translationally periodic array. No such array with the angle within 180 ± 2° was available in any of the three types of linkages.

If the angle 1-3-5, defined in the same manner as the angle 1-2-3, is close to 180°, one obtains a zig-zag array with 2_1 screw symmetry, as illustrated in Figure 8 *b*. There are 48 cases in which this angle is within 180 ± 2° in AB arrays. In the case of CD linkages, the angle is within 180 ± 2° in 37 arrays. The obvious next step was to combine each linear AB array with each CD array. There are 1776 such combinations. In the first step, just one array of one type was combined with one array of another type, as illustrated in Figure 9 *a*. Note that both the arrays emanated from the tetramer at the cross-section. As a rule of thumb, if two tetramers in the combination came closer than 50 Å or if two subunits belonging to two tetramers came closer than 30 Å, the combination was eliminated. In the first step, 840 of the 1776 combinations survived. Now two identical AB arrays were added to two identical CD arrays, as illustrated in Figure 9 *b*. When the distance criterion mentioned earlier was employed, only 257 combinations survived. Addition of a further array in each case led to further reduction in the allowed combinations (Figure 9 *c*), until the number in each set was four, as in Figure 9 *d*. Now the number of combinations reduced to two. Further addition of arrays of either type did not lead to reduction in the number of combinations. The crystal structures resulting from the two allowed combinations of AB and CD are illustrated in Figure 5 *a* and *b*. Interestingly, the CD array in both the structures is the same with $w1 = 60°$, $w2 = 180°$, $w3 = –90°$, $w4 = –90°$, $w5 = –60°$ and $w6 = –60°$. The AB arrays are different. One has torsion angles 60, 180, 90, 90, 180 and –60°. The torsion angles in the other are 180, 180, –90, –90, 180 and 180°. Both the structures have space group $P2_12_12_1$. The linked tetrameric molecules form a three-dimensional array in both the cases. The unit cell dimensions in one structure are $a = 260$ Å, $b = 91.6$ Å, $c = 100.4$ Å, while in the other they are $a = 260.8$ Å, $b = 100.0$ Å, $c = 98.6$ Å.

On account of symmetry, AC and BD arrays would coexist and would have identical linkages in each combination. There are 19 sugar conformations that lead to linear

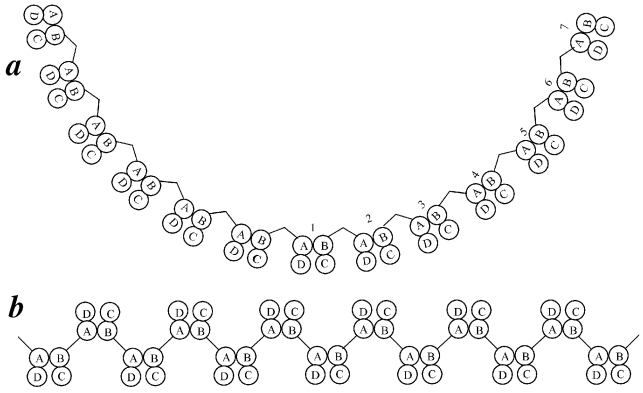

Figure 8. ***a***, Schematic representation of AB linked PNA tetramers. ***b***, Arrangement that results when the angle 1-3-5 is 180°. See text for details.

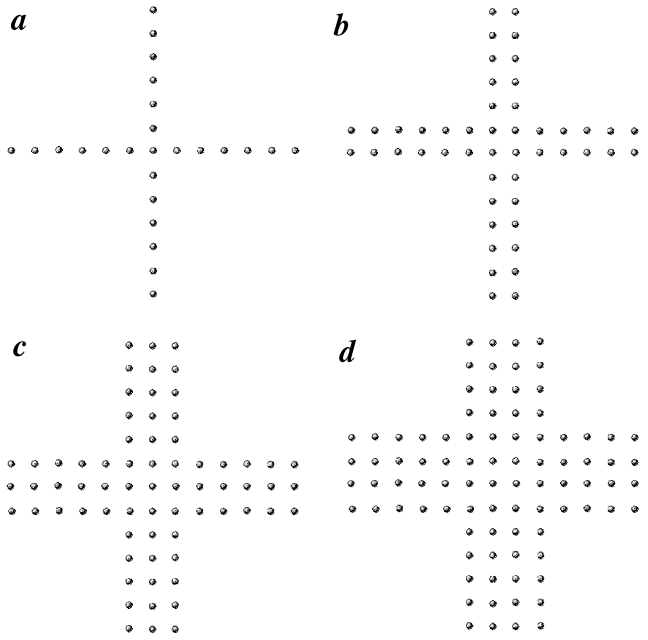

Figure 9. Schematic representation of construction of crystalline arrays involving AB (horizontal) and CD (vertical) linkages. See text for details.

arrays through AC linkages. Obviously, the same conformations also lead to linear BD arrays. However, when AC and BD arrays are combined, steric clashes resulted in every case. Therefore, crystalline arrays could not be generated using AC and BD linkages.

Rationalization of the crystal structure: The second objective of the modelling study was to rationalize the observed arrangement of linked molecules in the crystal structure. The crystalline arrays, which automatically resulted from modelling involving the ideal values of *w*1 to *w*6, did not correspond to the observed crystal structure. This is hardly surprising, as the conformational space was not exhaustively explored on account of computational limitations. If exhaustively explored, the arrangements appropriate for the crystal structure are likely to have been automatically found. Therefore, rationalization of the observed structure involved specifically looking for linkages appropriate for it, without resorting to a global search.

One of the terminal lactoses of LAL was positioned in the binding site of subunit A in tetramer AB′C′D in the crystal (Figure 4) and the positions of the other lactose were calculated for the 729 idealized conformations. The centroids of none of them came within 5 Å to the position of the centroid of the bound lactose in the B subunit of tetramer A′BCD′. Eight of them showed distances within 10 Å. If tetramer A′BCD′ is moved such that the position of the bound lactose in subunit B overlaps with the lactose molecule at the free ends of the eight conformers, severe steric contacts result in seven. The remaining one with torsion angles *w*1 to *w*6 of 60, –60, 60, –90, –60 and 180°, was chosen for further exploration. Each angle was varied within ± 30° at intervals of 10°. Of the 7^6 such conformers, the free lactose of eight came within 2 Å of the position of the bound lactose in the A′BCD′ tetramer. All these eight conformers had the same values of *w*1, *w*2 and *w*3 at 30, 70 and 60°; *w*4 ranged from 80 to 100°, *w*5 from 30 to 70°, and *w*6 from 160 to 170°. Each angle in these conformers was varied within ± 10° at 5° interval leading to a total of 73,250 finely spaced conformers. The lactose moiety in 405 of them came within 1 Å of the position of the bound lactose in the target subunit. In 11 of them, the lactose moiety makes all the hydrogen bonds observed in PNA–lactose complexes[16], with subunit B of tetramer A′BCD′, when a distance of 2.5–4.0 Å is considered to be appropriate for a hydrogen bond. These conformers are illustrated in Figure 6. The torsion angles in them fall within a narrow range of ± 15°. Any one of them could have been employed in the AB link in the crystal structure.

A similar exercise was carried out on the CD linkages. Only one conformer reproduced all the nine observed PNA–lactose hydrogen bonds. There were 27 others which reproduced seven of the nine hydrogen bonds. These 27 conformers also form a closely related set.

Concluding remarks

In the present investigation, cross-linking of PNA molecule by a bivalent molecule with lactose at the termini has been established in solution by dynamic light scattering and in the solid state by X-ray structure analysis. The formation, in the presence of LAL, of an apparent dimeric species and a larger aggregate involving about a hundred PNA molecules in solution is in consonance with the sequential, cooperative binding observed in thermodynamic measurements[21]. Detailed modelling studies provide a rationale for the observed arrangement of protein molecules in the crystal. Furthermore, modelling indicates the possibility of a number of different types of crystalline arrays produced by crosslinking. Thus, crosslinking involving multivalent lectins and multivalent carbohydrates could result in an ensemble of a finite number of distinct periodic arrays rather than a unique array. Such an ensemble may perhaps be better suited than a unique array to deal with the complexity and variability of glycoconjugates on the cell surface.

1. Lis, H. and Sharon, N., Lectins: carbohydrate-specific proteins that mediate cellular recognition. *Chem. Rev*., 1998, **98**, 637–674.
2. Vijayan, M. and Chandra, N., Lectins. *Curr. Opin. Struct. Biol*., 1999, **9**, 707–714.
3. Loris, R., Principles of structures of animal and plant lectins. *Biochim. Biophys. Acta*, 2002, **1572**, 198–208.
4. Bettler, H. M., Loris, R. and Imberty, A., Lectin database available online at http://cermav.cnrs.fr/lectines.
5. Brewer, C. F., Binding and crosslinking properties of galectin. *Biochim. Biophys. Acta*, 2002, **1572**, 255–262.

6. Drickamer, K.. Multiplicity of lectin carbohydrate interactions. *Nature Struct. Biol*., 1995, **2**, 437–439.
7. Brewer, C. F., Multivalent lectin–carbohydrate crosslinking interactions. *Chemtracts Biochem. Mol. Biol*., 1996, **6**, 165–179.
8. Brewer, C. F., Miceli, M. C. and Baum, L. G., Clusters, bundles, arrays and lattices: novel mechanisms for lectin–saccharide-mediated cellular interactions. *Curr. Opin. Struct. Biol*., 2002, **12**, 616–623.
9. Weis, W. I., Drickamer, K. and Hendrickson, W. A., Structure of a C-type mannose-binding protein complexed with an oligosaccharide. *Nature*, 1992, **360**, 127–134.
10. Bourne, Y. *et al.*, Crosslinking of mammalian lectin (galectin-1) by complex biantennary saccharides. *Nature Struct. Biol*., 1994, **1**, 863–870.
11. Olsen, L. R., Dessen, A., Gupta, D., Sabesan, S., Sacchettini, J. and Brewer, C. F., X-ray crystallographic studies of unique cross-linked lattices between four isomeric biantennary oligosaccharides and soybean agglutinin. *Biochemistry*, 1997, **36**, 15073–15080.
12. Sacchettini, J. C., Baum, L. G. and Brewer, C. F., Multivalent protein–carbohydrate interactions. A new paradigm for supermolecular assembly and signal transduction. *Biochemistry*, 2001, **40**, 3009–3015.
13. Wright, C. S. and Hester, G., The 2.0 Å structure of a cross-linked complex between snowdrop lectin and a branched mannopentose: evidence for two unique binding modes. *Structure*, 1996, **4**, 1339–1352.
14. Hamelryck, T. W., Moore, J. G., Chrispeels, M. J., Loris, R. and Wyns, L., The role of weak protein–protein interactions in multivalent lectin–carbohydrate binding: Crystal structure of cross-linked FRIL. *J. Mol. Biol*., 2000, **299**, 875–883.
15. Ramachandraiah, G., Chandra, N. R., Surolia, A. and Vijayan, M., Computational analysis of multivalency in lectin structures of garlic lectin-oligosaccharide complexes and their aggregates. *Glycobiology*, 2003, **13**, 765–775.
16. Banerjee, R., Das, K., Ravishankar, R., Suguna, K., Surolia, A. and Vijayan, M., Conformation of protein–carbohydrate interactions and a novel subunit association in the refined structure of peanut lectin-lactose complex. *J. Mol. Biol*., 1996, **256**, 281–296.
17. Ravishankar, R., Ravindran, M., Suguna, K., Surolia, A. and Vijayan, M., Crystal structure of the peanut lectin–T-antigen complex. Carbohydrate specificity generated by water bridges. *Curr. Sci*., 1997, **72**, 855–861.
18. Ravishankar, R., Suguna, K., Surolia, A. and Vijayan, M., Structure of the complexes of peanut lectin with methyl-*b*-galactose and *N*-acetyllactosamine and a comparative study of carbohydrate binding in Gal/GalNac specific legume lectins. *Acta Crystallogr. Sect. D*, 1999, **55**, 1375–1382.
19. Ravishankar, R., Thomas, C. J., Suguna, K., Surolia, A. and Vijayan, M., Crystal structures of the peanut lectin–lactose complex at acidic pH: retention of unusual quaternary structure, empty and carbohydrate bound combining sites, molecular mimicry and crystal packing directed by interactions at the combining site. *Proteins*, 2001, **43**, 260–270.
20. Natchiar, S. K., Jeyaprakash, A. A., Ramya, T. N. C., Thomas, C. J., Suguna, K., Surolia, A. and Vijayan, M., Structural plasticity of peanut lectin: an X-ray analysis involving variation in pH, ligand binding and crystal structure. *Acta Crystallogr. Sect. D*, 2004, **60**, 211–219.
21. Srinivas, O., Mitra, N., Surolia, A. and Jayaraman, N., Photoswitchable multivalent sugar ligands: synthesis, isomerization, and lectin binding studies of azobenzene–glycopyranoside derivatives. *J. Am. Chem. Soc*., 2002, **124**, 2124–2125.
22. Srinivas, O., Mitra, N., Surolia, A. and Jayaraman, N., Photoswitchable cluster glycosides as tools to probe carbohydrate–protein interactions: synthesis and lectin-binding studies of azobenzene containing multivalent sugar ligands. *Glycobiology*, 2005, **15**, 861–873.
23. Otwinowski, Z., In Proceedings of the CCP4 Study Weekend. Data Collection and Processing (eds Sawyer, L. *et al.*), Daresbury Laboratory, Warringtom, 1993, pp. 56–62.
24. CCP4 (Collaborative Computational Project, No. 4). *Acta Crystallogr. Sect. D*, 1994, **50**, 760–763.
25. Navaza, AMoRe: an automated package for molecular replacement. *Acta Crystallogr. Sect. A*, 1994, **50**, 157–163.
26. Cohen, G. E., ALIGN: a program to superimpose protein coordinates, accounting for insertions and deletions. *J. Appl. Crystallogr*., 1997, **30**, 1160–1161.
27. DeLano, L. W., The case for open-source software in drug discovery. *Drug Discovery Today*, 2005, **10**, 213–217.
28. Kraulis, P. J., MOLSCRIPT: a program to produce both detailed and schematic plots of protein structures. *J. Appl. Crystallogr*., 1991, **24**, 946–950.
29. Lee, K. K. and Johnson, J. E., Complementary approaches to structure determination of icosahedral viruses. *Curr. Opin. Struct. Biol*., 2003, **13**, 558–569.
30. Orlova, E. V. and Saibil, H. R., Structure determination of macromolecular assemblies by single-particle analysis of cryo-electron micrographs. *Curr. Opin. Struct. Biol*., 2004, **14**, 584–590.
31. Berman, H. M. *et al.*, The protein data bank. *Nucleic Acids Res*., 2000, **28**, 235–242.

ACKNOWLEGDEMENTS. X-ray intensity data were collected at the X-ray Facility for Structural Biology supported by the Department of Science and Technology (DST) and Department of Biotechnology (DBT), New Delhi. Computations were carried out at the Supercomputer Education and Research Centre and the Bioinformatics Centre and Graphics Facility, IISc supported by DBT. Financial assistance from DST is acknowledged. M.V. is supported by a Distinguished Biotechnology Award of the DBT.

Received 2 February 2006; revised accepted 1 April 2006